ChemPlusChem

A Multidisciplinary Journal Centering on Chemistry

Chemistry Europe

European Chemical Societies Publishing

Accepted Article

Title: A Study on Thiol-Michael Addition to Semi-Synthetic Elastin-Hyaluronan Material for Electrospun Scaffolds

Authors: Antonio LAEZZA, Antonietta Pepe, Nicola Solimando, Francesca Armiento, Floriane Oszust, Laurent Duca, and Brigida Bochicchio

To be cited as: *ChemPlusChem* **2024**, e202300662

Link to VoR: https://doi.org/10.1002/cplu.202300662

WILEY VCH

10.1002/cplu.202300662

RESEARCH ARTICLE

WILEY VCH

A Study on Thiol-Michael Addition to Semi-Synthetic Elastin-Hyaluronan Material for Electrospun Scaffolds

Antonio Laezza,[a] Antonietta Pepe,[a] Nicola Solimando,[b] Francesca Armiento,[a] Floriane Oszust,[c] Laurent Duca,[c] and Brigida Bochicchio*[a]

[a] Dr. A. Laezza, Prof. A. Pepe, F. Armiento, Prof. B. Bochicchio
Department of Science
University of Basilicata
Viale dell'Ateneo Lucano 10, 85100, Potenza (Italy)
E-mail: brigida.bochicchio@unibas.it

[b] N. Solimando
Altergon Italia S.r.l.
Zona Industriale ASI, Morra De Sanctis, 83040, Italy

[c] F. Oszust, Prof. L. Duca
MEDyC UMR CNRS 7369, "Matrice Extracellulaire et Dynamique Cellulaire"
University of Reims Champagne-Ardenne, Team 2 "Matrix Ageing and Vascular Remodelling"
51100, Reims, France

Supporting information for this article is given via a link at the end of the document.

Abstract: Thiol-Michael addition is a chemical reaction extensively used for conjugating peptides to polysaccharides with applications as biomaterials. In the present study, for designing a bioactive element in electrospun scaffolds as wound dressing material, a chemical strategy for the semi-synthesis of a hyaluronan-elastin conjugate containing an amide linker (ELAHA) was developed in the presence of tris(2-carboxyethyl)phosphine hydrochloride (TCEP·HCl). The bioconjugate was electrospun with poly-D,L-lactide (PDLLA), obtaining scaffolds with appealing characteristics in terms of morphology and cell viability of dermal fibroblast cells. For comprehending the factors influencing the efficiency of the bioconjugation reaction, thiolated amino acids were also investigated as nucleophiles toward hyaluronan decorated with Michael acceptors in the presence of TCEP·HCl through the evaluation of byproducts formation.

Introduction

Peptide-polymer conjugates are attractive materials in biomedical applications,[1] ranging from drug discovery and delivery to tissue engineering. The bioconjugates show enhanced properties in comparison to peptides alone, which show sensitivity to organic solvents, temperature and pH. Among naturally sourced polymers, polysaccharides, are strongly appealing for conjugation with peptides due to their biocompatibility and biodegradability characteristics.[2]

Considering the different chemical strategies for polysaccharides-peptide conjugation,[2b],[3] the Michael-type addition has been widely used for the advantageous mild reaction conditions, high reactivity and bio-orthogonality.[4]

In this reaction, thiols react with electron-poor "ene" groups such as acrylates, methacrylates and methacrylamidates under basic conditions without requiring free radicals and affording derivatives with stable thioether bonds. Typically, the thiol groups are inserted into peptide chains through cysteine residues at a specific position, whereas Michael acceptor "ene" groups consist of a suitably decorated polysaccharide backbone.[2b]

Although acrylates are more reactive than methacrylates into thiol-Michael addition, the hydrolysis resistance of their adducts is reduced in comparison with the methacrylate ones,[4] which in turn are more sensitive to the hydrolysis respect to the methacrylamide counterparts.[5]

In the field of wound healing, materials relying on the cleavage of chemical bonds under the influence of pH for a precise drug delivery to wounded sites are continuously under study.[6]

Moreover, for the treatment of wounds, the design of materials inspired by the extracellular matrix (ECM) components, such as elastin and hyaluronan (HA), is intriguing. As a matter of fact, systems composed of HA and elastin have been developed for tissue engineering, such as films and hydrogels,[7] and their application specifically in wound healing is still limited.[8]

The fibrous elastin protein is responsible for the resilience and elastic recoil of tissues lost after a skin injury. Analogously, the glycosaminoglycan (GAG) plays several roles in the processes after a skin injury, from the hemostasis to the remodelling.[9]

Regarding the fabrication methodology, the electrospinning process allowed the production of nanofibrous biomaterials possessing a beneficial porous structure with a high surface-to-volume ratio. Air and water transport, characteristics of electrospun fibers, allows a moist environment fundamental for cell proliferation, lowering the chance of infection. On the other hand, porous structure reproduces the tridimensionality of ECM, facilitating cell adhesion, migration, and proliferation.[10]

In the last decades, the interest towards producing nonwoven fabrics obtained from recombinant and synthetic sourced elastin

for wound treatment has grown[11] since these materials have exhibited good cell colonization. Electrospun elastin scaffolds reported poor contraction after cell colonization, differently from collagen ones, which reported, in some cases, a reduction larger than 50% of the original size.[12] As other ECM component, HA is conveniently usable in creating electrospun nanofibers for wound healing due to its influence on inflammation, cell migration and proliferation, angiogenesis, and re-epithelialization processes.[13] However, HA aqueous solutions' high viscosity and surface tension impair the electrospinning of this polysaccharide in its natural conditions and by itself. Many strategies have been applied to overcome this drawback, including using organic solvent mixtures, blending HA with other polymers and its backbone modification.[14]

The insertion of methacrylate, acrylate or thiol pending groups on HA[7c,15] for a Michael-type reaction has been reported, either at the carboxylic function of D-glucuronic acid (GlcA) or at primary hydroxyl of the *N*-acetyl-D-glucosamine (GlcNAc) units of the glycosaminoglycan. The subsequent coupling has been usually carried out with a subsequent coupling with a cysteine [16] or with a Michael-acceptor-containing peptide,[17] respectively.

Based on the skills acquired in amino acids,[18] peptides,[19] and protein[20] conjugation to carbohydrates, and starting from the semi-synthesis of ELAHA, herein we present a study exploiting the reactivity of methacrylamide and methacrylate linkers in the presence of a water-soluble alkylphosphine such as TCEP·HCl. This latter is typically employed both as a catalyst[21] and as reducing agent[22] in bioconjugation reactions, even though its efficiency is controversial. Several examples of low functionalization, for example, have been reported in the presence of maleimide, suggesting a possible side reaction between TCEP·HCl and thiol-Michael type donor.[23]

Herein, we have explored the feasibility of Micheal-type thiol-ene reaction for the production of a bioconjugate constituted of an elastin-derived peptide grafted to hyaluronic acid. The final product would benefit biocompatibility and bioactivity properties as well. In this work, a methacrylamide moiety has been inserted into the glycosaminoglycan carboxylic function on GlcA unit. The obtained methacrylamide-decorated hyaluronan derivative (MAAHA), based on the conditions reported in our recent work[19a], has been covalently conjugated in the presence of alkylphosphine to the peptide corresponding to the region 302-322 of human tropoelastin (HTE) promoting cell attachment and spreading.[24] The sequence of the peptide (C)AAAAAAAAAAKAAKYGAAAGL (**1**) after the insertion of a cysteine at the C-terminus to carry out Michael-type addition. The nonquantitative bioconjugation between **1** and MAAHA has encouraged us to investigate and compare the efficiency of the Michael addition reaction of MAAHA and a methacrylate-decorated hyaluronan (MAHA) with L-cysteine (Cys) and *N*-acetyl-L-cysteine (NAcCys) amino acids.

The semi-synthetic derivatives were characterized by nuclear magnetic resonance (NMR), attenuated total reflectance Fourier transform infrared (ATR-FTIR) spectroscopy and then electrospun with racemic PDLLA to obtain scaffolds, whose morphology was investigated by scanning electron microscopy (SEM).

Finally, with the perspective of applications as wound dressing materials, the electrospun scaffolds underwent a cytotoxic analysis and were compared with the ones containing bioconjugates obtained from MAHA polysaccharide.

Results and Discussion

Semi-synthesis of polysaccharide derivatives

The strategy for semi-synthesizing elastin-hyaluronan glycoconjugate, exploiting thiol Michael-type addition, started with the amidation at the carboxyl group of GlcA unit of HA by the insertion of methacrylamide moiety. This was accomplished in water in the presence of 2-aminoethylmethacrylamide hydrochloride (2-AEMAA·HCl), *N*-(3-(dimethylamino)propyl)-*N*'-ethylcarbodiimide reagent (EDC·HCl) and *N*-hydroxysulfosuccinimide (s-NHS) at pH=6.8, (Scheme 1, a). After overnight reaction at room temperature, dialyses and subsequent freeze-drying furnished MAAHA derivative **2** in quantitative mass yield and with a degree of substitution ($DS_{methacryl}$) of 0.30, as calculated by ^{1}H-NMR (Figure 1).

The amide bond formation in MAAHA (**2**) was confirmed by ^{1}H-NMR spectrum for the presence of signals at δ_{DSS} = 1.91 ppm, δ_{DSS} = 5.69 ppm, and δ_{DSS} = 5.45 ppm, respectively associated to the $-CH_3$, and $=CH_2$ groups, of methacrylamide linker. The $DS_{methacryl}$ of derivative **2** was calculated by comparing the ^{1}H-NMR vinyl (δ_{DSS} = 5.69, or 5.44 ppm) integrals with that obtained by the sum of HA and 2-AEMAA acetyl signals (δ_{DSS} =2.01 and 1.91 ppm) (Figure S1) by Equation (1)

$$DS_{methacryl} = \frac{3I_{CH(2-AEMAA)}}{I_{[CH_3(GlcNAc)+CH_3(2-AEMAA)]} - 3I_{CH\ (2-AEMAA)}} \quad (1)$$

where *I*CH(2-AEMAA) represents the proton integral of the 2-AEMAA methine proton, while *I*CH_3(GlcNAc) and *I*CH_3(2-AEMAA) represent the proton integrals of the methyl groups of GlcNAc and 2-AEMAA, respectively.

Derivative **2** was coupled to the cysteine thiol at the *N*-terminal residue of elastin-derived peptide **1** (Scheme 1, b) to obtain ELAHA (**3**).

The ^{1}H-NMR of this compound (Figure 1, blue) showed a nonquantitative functionalization by the presence of 2-AEMAA groups, such as the methyl at δ_{DSS} = 1.91 ppm and the smaller vinyl signals, which entail respectively a $DS_{methacryl}$ = 0.06 and a $DS_{addition}$ = 0.24. The latter has been calculated by the difference of vinyl signals intensity after and before the coupling. The bioconjugation was confirmed further by the peptide side chain signals, such as the $-CH_3$ groups of alanine and leucine residues, respectively, at δ_{DSS} = 1.54–1.30 ppm, δ_{DSS} = 0.91, and δ_{DSS} = 0.86 ppm.

The reactivity of acceptors into the thiol-Michael addition is related to the electronic feature of the substituent linked to the C=C bond:[25] at any given pH the reaction proceeds rapidly with acceptors bearing esters, slower with amides or methacrylates. In contrast, the slowest rates were calculated for methacrylamides, due to the poor electronegativity of amides.[26]

Therefore, to evaluate how the coupling conditions affected ELAHA semi-synthesis, two thiols such as Cys and NAcCys, were studied as donors in the presence of MAAHA (**2**) or MAHA (**4**) as acceptors (Figure 2).

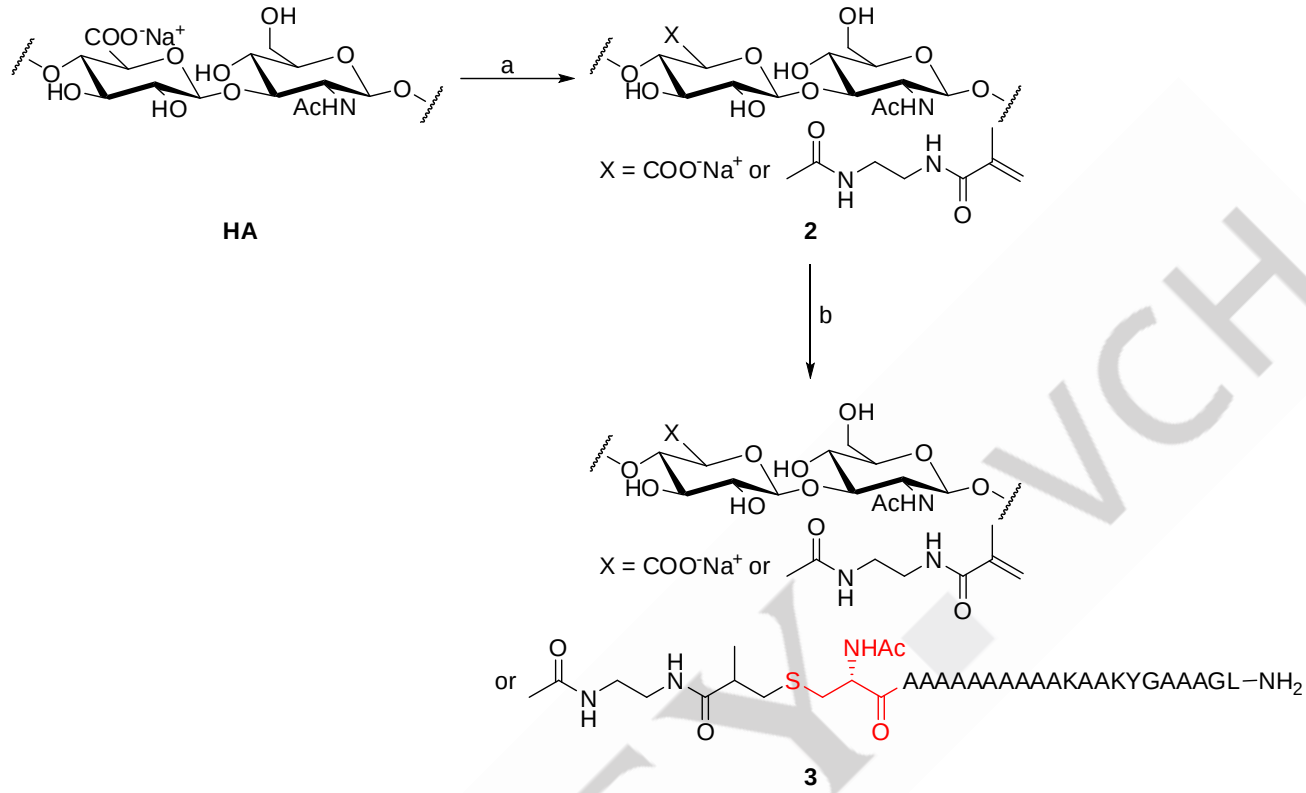

Scheme 1. Semi-synthesis of derivative **3**.a) 2-AEMAA·HCl, EDC, s-NHS, H_2O, RT, pH = 6.8, overnight, yield = 79%, $DS_{methacryl}$ = 0.30; b) **1**, TCEP·HCl, H_2O, RT, pH = 8.9, 2d, yield = 41%, $DS_{methacryl}$ = 0.06, $DS_{addition}$ = 0.24.

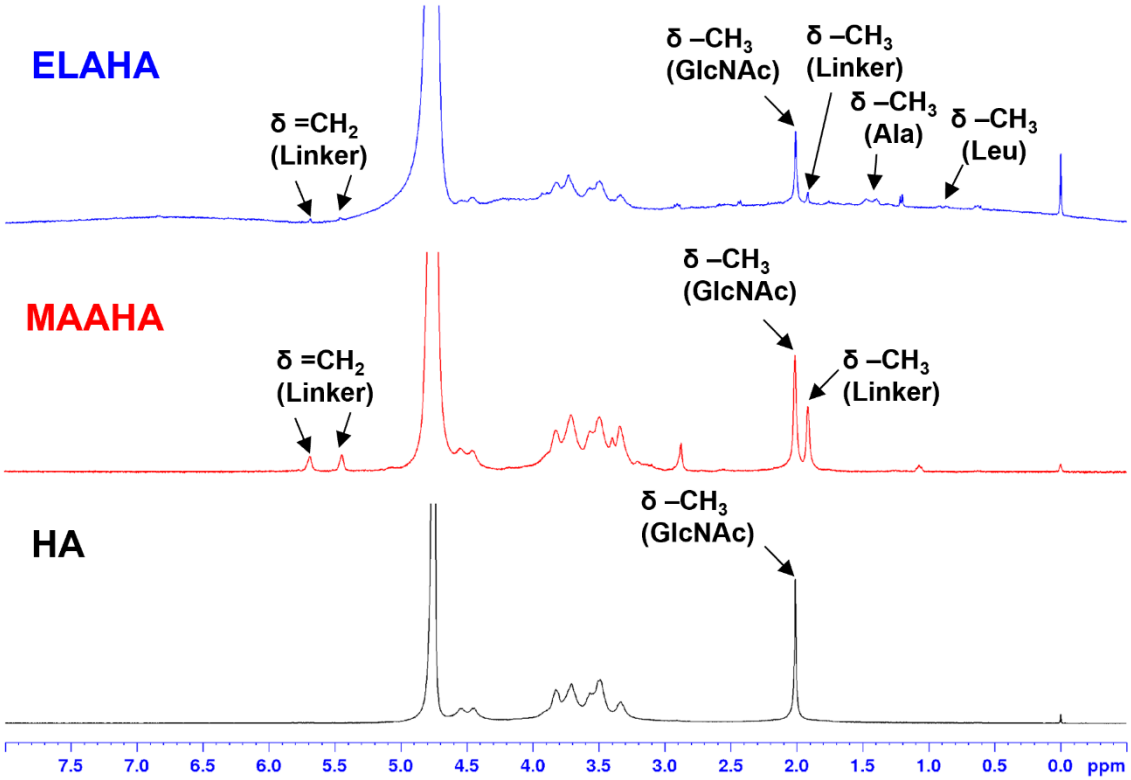

Figure 1. ^{1}H-NMR spectra of HA (black), derivative **2** (MAAHA, red), and derivative **3** (ELAHA, blue) (400 MHz, D_2O, 298 K)

MAHA has been synthesized under conditions recently reported[19a] with a $DS_{methacryl}$ = 0.19 (Figure S2).

All the reactions were carried out for two days at room temperature in H_2O at pH = 8.9, where the acceptor/donor/nucleophile ratios investigated were 1:1.3:1.9 and 1:1.5:2.25, as reported in Table 1. The conjugation of Cys with MAAHA$_T$ afforded derivatives **5-i,ii** (Scheme 2a,b) in 77% and 41% mass yield.

Analogously with ELAHA, they showed a nonquantitative functionalization by the presence of 2-AEMAA groups, which entail a $DS_{methacryl}$ = 0.13 and 0.06 and a $DS_{addition}$ = 0.17 and 0.24, for **5-i** and **5-ii**, respectively (Figure S3, red and blue curves).

The reactivity of Cys with the acceptor MAHA afforded derivatives **6-i,ii** (Scheme 2c,d). In this case a disappearance of vinyl signals was noted and a $DS_{addition}$ = 0.19 (Figure S4, red and blue curves) was obtained for both the compounds, which were collected in 68% and 50% mass yield.

Michael donors

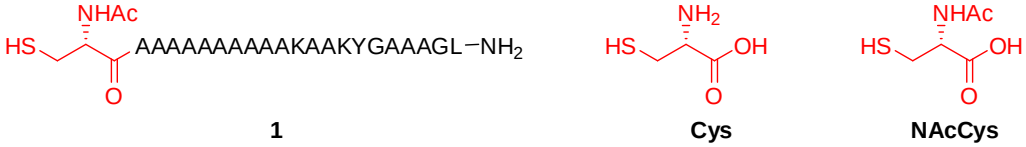

1 **Cys** **NAcCys**

Michael acceptors

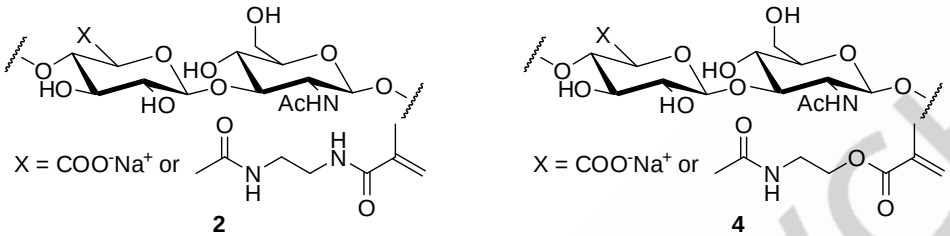

Nucleophile catalyst

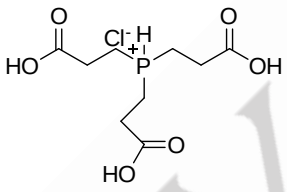

TCEP•HCl

Figure 2. Michael donors, acceptors and nucleophile catalyst used in the study

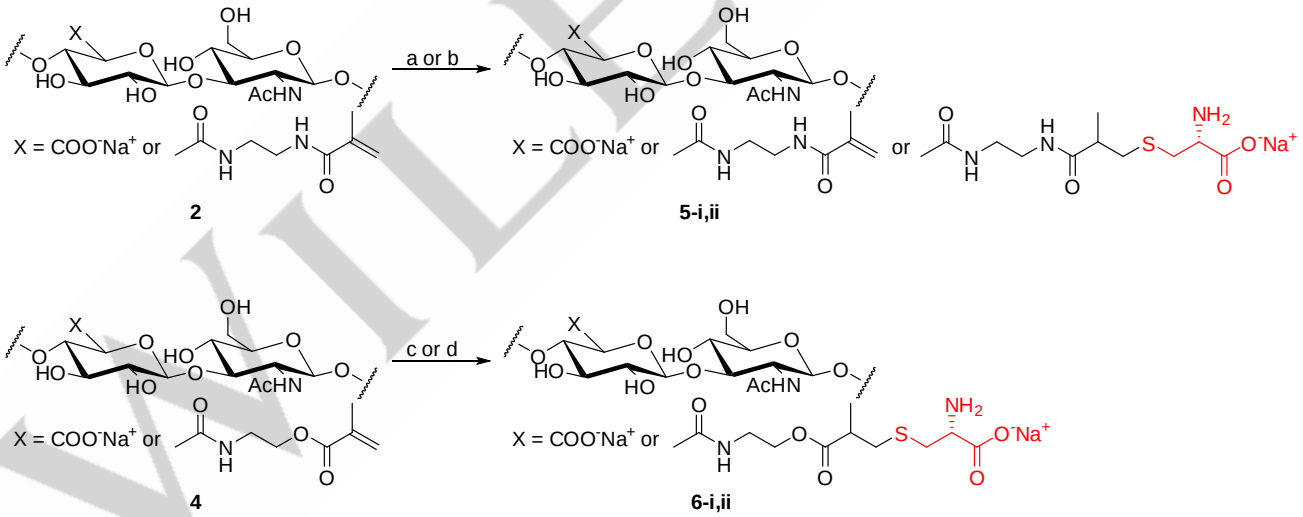

Scheme 2. Cys investigation as Michael donor: a) Cys (1.3 eq), TCEP·HCl (1.9 eq), H_2O, RT, pH = 8.9, 2d, yield: 77%, $DS_{methacryl}$ = 0.13, $DS_{addition}$ = 0.17; b) Cys (1.5 eq), TCEP·HCl (2.25 eq), H_2O, RT, pH = 8.9, 2d, yield: 41%, $DS_{methacryl}$ = 0.06, $DS_{addition}$ = 0.24; c) Cys (1.3 eq), TCEP·HCl (1.9 eq), H_2O, RT, pH = 8.9, 2d, yield: 68%, $DS_{addition}$ = 0.19; d) Cys (1.5 eq), TCEP·HCl (2.25 eq), H_2O, RT, pH = 8.9, 2d, yield: 50%, $DS_{addition}$ = 0.19.

The presence in peptide **1** of the L-cysteine, acetylated at the amino group in the final step of SPPS, suggested us to employ *N*-acetyl-L-cysteine as a model amino acid playing the role of a donor. The conjugation of NAcCys with MAAHA afforded derivatives **7-i,ii** (Scheme 3a,b) respectively in 44% and 57% mass yield and with a $DS_{methacryl}$ = 0.07 and a $DS_{addition}$ = 0.23 as calculated by ^{1}H-NMR (Figure S5, red and blue curves) applying Equation (2).

$$DS_{methacryl} = \frac{3I_{CH(2-AEMAA)}}{I_{[CH_3(GlcNAc)+\,CH_3(NAcCys)+\,CH_3(2-AEMAA)]} - 6I_{CH\,(2-AEMAA)}} \quad (2)$$

When NAcCys reacted with MAHA (Scheme 3c,d), derivatives **8,i-ii** were respectively obtained in 91% and 86% mass yield

with a quantitative functionalization and a $D_{Saddition}$ = 0.19 (Figure S6, red and blue curves).

However, the absence of isolated protons ascribable to the thiolated amino acids did not allow the evaluation of functionalization; for this reason, correlation spectroscopy 2D-NMR (COSY) analyses were conducted. The derivatives obtained after Cys bioconjugation (Figures S7-S10) displayed a correlation between the methylene protons density at δ_{DSS} = 3.11 and that at δ_{DSS} = 3.93 in the typical region of the H_α proton of the thiolated amino acid, suggesting its presence on the polysaccharide backbone.

In the case of NAcCys bioconjugation (Figures S11-S13), a correlation was detected between the methylene protons at δ_{DSS} = 2.88 and the H_α proton of the amino acid at δ_{DSS} = 4.37 ppm. The exception is represented by the sample **8-i**, where the presence of NAcCys is not evident (data not shown). In both cases, the upfield shift of H_α amino acids might suggest the Michael addition occurrence.[27]

Moreover, the depletion of vinyl signals does not exclude the presence of side products formed in the thiol-Michael reactions. ^{1}H-NMR spectra of the amino acid-hyaluronan derivatives, indeed, displayed signals in the region 2.70 -2.00 ppm, possibly related to contaminants; therefore, ^{31}P-NMR experiments were conducted to evaluate the presence of undesired products. The same analysis was conducted on ELAHA, which displayed the absence of any signal related to phosphorus adducts (Figure S14).

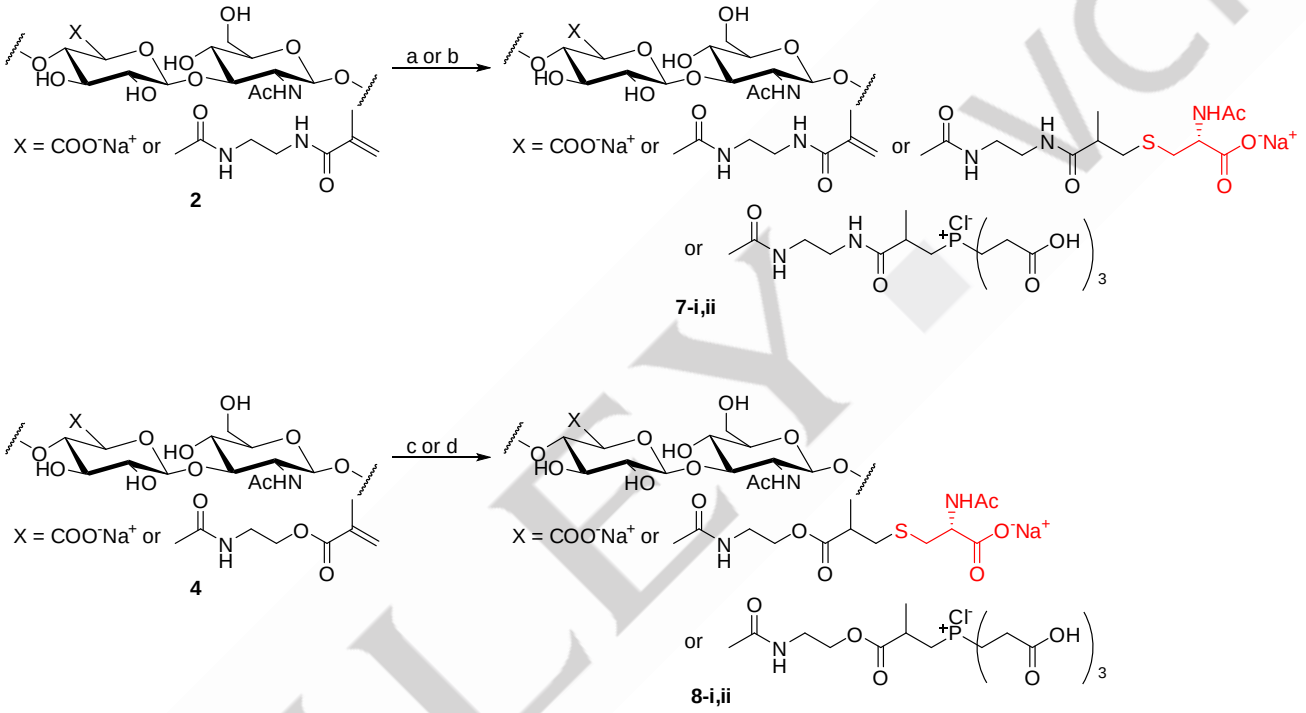

Scheme 3. NAcCys investigation as Michael donor: a) NAcCys (1.3 eq), TCEP·HCl (1.9 eq), H_2O, RT, pH = 8.9, 2d, yield: 44%, $DS_{methacryl}$ = 0.07, $DS_{addition}$ = 0.23; b) NAcCys (1.5 eq), TCEP·HCl (2.25 eq), H_2O, RT, pH = 8.9, 2d, yield: 57%, $DS_{methacryl}$ = 0.07, $DS_{addition}$ = 0.23; c) NAcCys (1.3 eq), TCEP·HCl (1.9 eq), H_2O, RT, pH = 8.9, 2d, yield: 91%, $DS_{addition}$ = 0.19; d) NAcCys (1.5 eq), TCEP·HCl (2.25 eq), H_2O, RT, pH = 8.9, 2d, yield: 86%, $DS_{addition}$ = 0.19.

Regardless of the acceptor and the reaction conditions, the conjugations with Cys showed two phosphorus signals at δ_{DSS} = 58.2 ppm and δ_{DSS} = 52.8 ppm, consistent with oxidized (TCEP=O) and the thiophosphine byproducts (TCEP=S), respectively (Figure S15-S16).[28] These confirmed the absence of hyaluronan-phosphine adducts (**5-i,ii** and **6-i,ii**, Scheme 2). A different behavior has been noted with the NAcCys conjugation, where the formation of phosphonium ester adducts has been detected. In the case of the MAAHA acceptor, the adduct has formed independently from the equivalents of the catalyst and the ^{31}P-NMR spectra (Figure S17) showed a signal at δ_{DSS} = 34.5 in agreement with literature data.[29] When the same reaction was conducted on MAHA, the formation of phosphonium ester was dependent on the equivalent of the catalyst (Figure S18). The ^{31}P-NMR spectra showed signals in the range of δ_{DSS} = 34.7 – 33.6 ppm: these signals could be associated with a different protonation level of the phosphorus adduct (**7-i,ii** and **8-i,ii**, Scheme 3).[30]

Cys is more acidic than NAcCys; hence, the thiol group is mainly present as more nucleophilic thiolate at the given pH. However, a selectivity for the Cys is evident in the addition on the methacrylate and on the methacrylamide acceptors.

Besides the thiol/thiolate ratio,[26] a combination of vinyl, catalyst and reaction conditions[31] influences the reaction mechanism. Because of the higher electron-withdrawing capability, the methacrylate is more reactive than the methacrylamide, which could be generally affected by the formation of byproducts for the competition of nucleophile initiator with the thiolate.

It is worth noting that the pH plays a pivotal role in the reaction efficiency. In the cysteine-containing derivatives, the phosphonium ester side products are absent due to the faster addition kinetic to the vinyl groups of the thiolate than the

phosphine; the only difference in the conjugation could be attributed to the electron-withdrawing feature of the acceptors.
Notably, despite the different acceptors' electrophilicity, when NAcCys has been used as a model, the byproducts formation is influenced by the higher thiol/thiolate ratio by the excess of phosphine catalyst. These findings confirm the controversial role of TCEP·HCl in the catalysis of thiol-Michael addition on polysaccharides.[32] Generally, organophosphines can be considered efficient catalysts in the thiol-Michael addition, even if their high reactivity tends to induce side reactions. In recent years, several theoretical and experimental approaches have been adopted to deepen the factors involved in the nucleophilic pathway and in the generation of byproducts.[27b,33]

Table 1 Coupling conditions, yield and structural data of derivatives **5-8** in the thiol-Michael addition study.

Sample	Acceptor	Donor	Acceptor/Donor/Nucleophile Ratio	Donor/Nucleophile Ratio	Yield	$DS_{methacryl}$	$DS_{addition}$
3	MAAHA	EL	1:1.3:1.9	1:1.5	41%	0.06	0.24
5-i	MAAHA	Cys	1:1.3:1.9	1:1.5	77%	0.13	0.17
5-ii	MAAHA	Cys	1:1.5:2.25	1:1.5	41%	0.06	0.24
6-i	MAHA	Cys	1:1.3:1.9	1:1.5	68%	-	0.19
6-ii	MAHA	Cys	1:1.5:2.25	1:1.5	50%	-	0.19
7-i	MAAHA	NAcCys	1:1.3:1.9	1:1.5	44%	0.07	0.23
7-ii	MAAHA	NAcCys	1:1.5:2.25	1:1.5	57%	0.07	0.23
8-i	MAHA	NAcCys	1:1.3:1.9	1:1.5	91%	-	0.19
8-ii	MAHA	NAcCys	1:1.5:2.25	1:1.5	86%	-	0.19

ATR-FTIR Analysis

The characterization of HA, MAAHA and ELAHA was further carried out by ATR-FTIR (Figure S19), allowing the assignment of specific functional groups on the polysaccharide backbones. HA spectrum (black curve) shows in the 3500–3000 cm^{-1} region a broad band attributed to the stretching of carbohydrate O-H, as well as, C=O (amide I, filled green circle) and C-N (amide II, filled orange circle) bands of acetamido groups stretching vibrations are observed at ~ 1605 and ~ 1550 cm^{-1}, respectively. Derivative **2** spectrum (MAAHA, red curve), proved the occurrence of methacrylamidation by the slight shift peak of the amide I band (filled green circle) to ~ 1610 cm^{-1} caused by the inductive effect of the methyl group of the linker.
Several findings confirmed the peptide presence in derivative **3** (ELAHA, blue curve). First of all, the sharpening of the band at ~ 3269 cm^{-1} due to N-H stretching (filled blue circle) of the peptide amide is evident. It appears in the same region where the O-H stretching of pristine HA (black curve) and the derivative **2** (MAAHA, red curve) were present as a broad band at ~ 3281 cm^{-1}.
Moreover, the amide I band (filled green circle) is shifted to ~ 1622 cm^{-1}. This one, together with the amide II band at ~ 1516 cm^{-1} (filled orange circle) are assigned to the peptide **1**.
Further proof derives from the band at ~ 1450 cm^{-1} (filled gray circle) in the purple curve associated with the asymmetric C-H_3 bending vibration of alanine residues, which are present in peptide **1** spectrum (purple curve) and absent in HA and derivative **2** curves.

Morphological Analysis

HA, derivatives **2** and **3** were blended with PDLLA and electrospun, with the process parameters listed in Table 2, fulfilling the aim to produce electrospun scaffolds made of biodegradable and bioactive polymers. 1,1,1,3,3,3-hexafluoro-2-propanol (HFP) was chosen because of its ability to solubilize both elastin peptides and PDLLA as pure solvent[34] and in aqueous solutions.[19a] The electrospinning parameters were tuned to ensure process stability, providing macroscopically uniform structures. Herein, to dissolve HA, derivatives **2** and **3**, HFP was mixed with H_2O: HP (HA/PDLLA), MAHP (MAAHA/PDLLA) and EAHP (ELAHA/PDLLA) blends were prepared by dissolving in 80% (V/V) HFP aqueous solution either HA, MAAHA or ELAHA and PDLLA to a final concentration of 0.24% and 12.0% (w/V), respectively. In the same way, the P scaffold, containing pristine PDLLA, was prepared by dissolving the polymer in 80% (V/V) HFP aqueous solution to a final concentration of 12.0% (w/V).
Scanning electron microscopy investigated the morphology of the scaffolds with particular attention to the assessment of any defect (beads), the fibers' orientation, and the diameter distribution.
Concerning the detection of beads, the SEM image of the electrospun P scaffold (Figure 3A) showed a three-dimensional microstructure enriched with interconnected pores and bead-on-string morphology that typically arises when the surface tension of the liquid overcomes the charge repulsion and viscous forces.[35]

Table 2 Composition, process parameters and morphology of electrospun scaffolds

Scaffolds[a]	Composition	Polymer weight ratio (w/w)	Final polymer concentration % (w/V)	Electrospinning process parameters				Average fiber diameter[b] (nm)
				V (kV)	N (G)	d (cm)	F (mL/h)	
P[c]	PDLLA	-	12.00	19	18	19	0.5	448 ± 121
HP[c]	HA/PDLLA	1:50	12.24	19	18	19	0.5	417 ± 34
MAHP	MAAHA/PDLLA	1:50	12.24	19	18	19	0.5	410 ± 8
EAHP	ELAHA/PDLLA	1:50	12.24	19	18	19	0.5	456 ± 17

[a] P: (poly-lactic acid), HP: (hyaluronic acid/poly-lactic acid), MAHP: (methacrylamidated hyaluronic ac-id/poly-lactic acid), EAHP: (elastin-conjugated hyaluronic acid/poly-lactic acid), [b] Mean value ± standard deviation (n>100 from three different images). [c] Average fiber diameter of P and HP are taken as a reference from [19a].

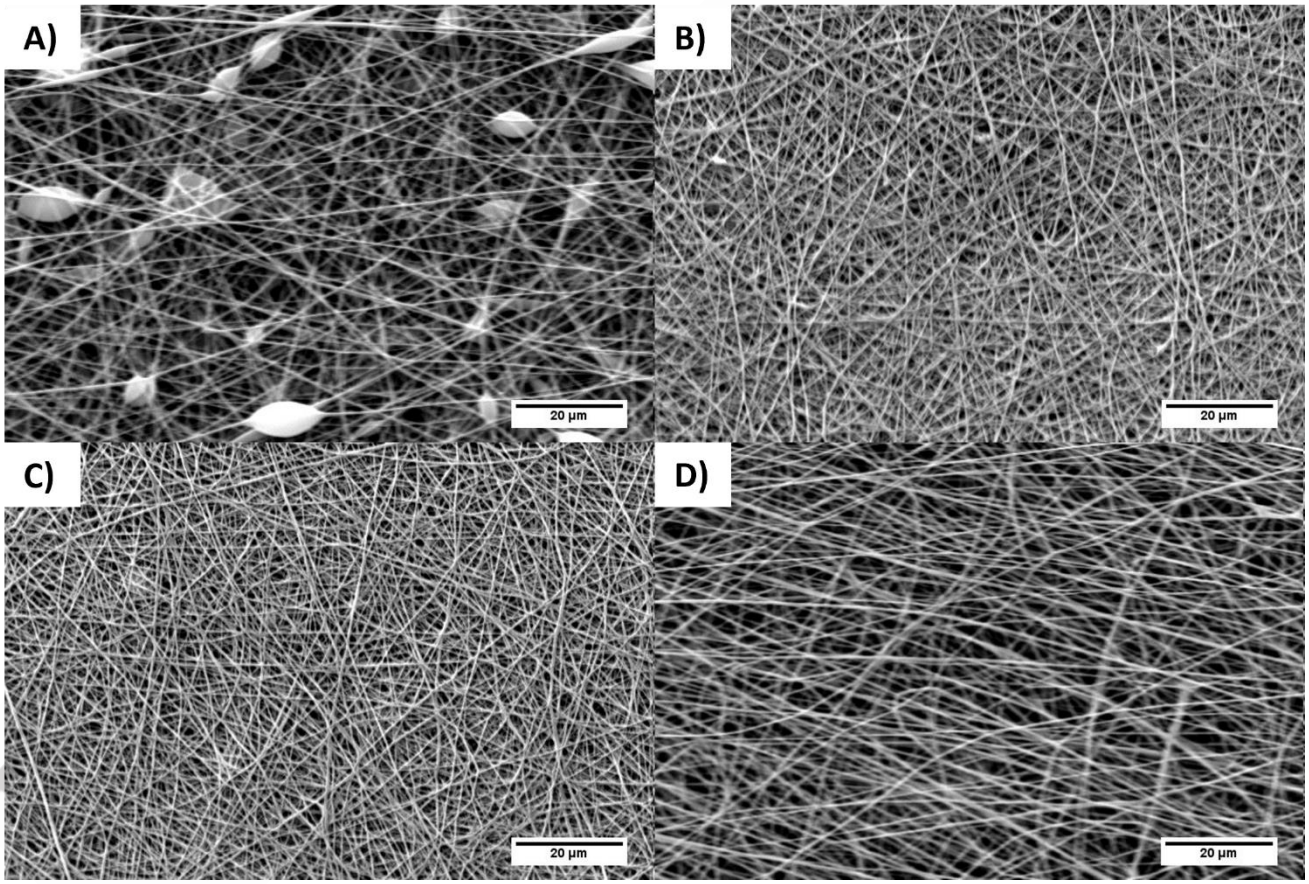

Figure 3. SEM images of electrospun scaffolds. P (A), HP (B), MAHP (C), EAHP (D); (bar: 20 µm). Images A and B are taken from [19a]

Generally, the surface tension and viscosity of the electrospinnable mixture depend on the polymer and the solvent system used, as well as the charge density is dependent on the applied voltage. The presence of H_2O increases the surface tension as opposed to pure HFP solution, leading to beads formation in the nanofibrous morphology.[36] Nevertheless, HP, MAHP and EAHP scaffolds displayed fibers with a linear trend, without beads, suggesting an increase of electrospun solution viscosities, differently from the scaffold P solution, and the effective dispersion of the polysaccharides and semi-synthetic derivatives in the mixture due to the absence of defects (Figure 3B-D). Moreover, for EAHP scaffold, the fibers appeared slightly curled. The average diameters of fibers as function of frequency (Figures S20A–B) showed a normal distribution around a mean

value of 448 ± 121, 417 ± 34, 410 ± 8, and 456 ± 17 nm for P, HP, MAHP, and EAHP electrospun scaffolds, respectively, as reported in Table 2.

The differences in the fibers' diameter between the scaffolds were evaluated by statistical analyses using the one-way Analysis of Variance (ANOVA) method and Tukey's Test. Between P and HP as well as P and MAHP membranes, a significant decrease was observed for *p ≤ 0.05 (from 448 ± 121 to 417 ± 34, and from 448 ± 121 to 410 ± 8), whereas for **p ≤ 0.01 a statistical reduction in average diameter was found by comparison of P and MAHP membranes (Figure S21) (from 448 ± 121 to 410 ± 8). Even though by blending HA and MAAHA with PDLLA, the viscosity of the solution should rise, with a relative increase of nanofibers diameter, the observed data could be the results of humidity increasing, which allows elongation of the charged jet to continue longer and thereby to form thinner fibers.[37] However, the substantial standard deviation (SD) related to the measure of scaffold P should be taken into account due to bead formation.

Differently from previous studies,[19a] in the case of EAHP scaffold, the presence of ELAHA glycoconjugate induced a significant increase of average fibers diameter with *p ≤ 0.05 and **p ≤ 0.01 respect to HP and MAHP, as reported in Table 2 (from 417 ± 34 to 456 ± 17, and from to 456 ± 17, respectively). Since P, HP, MAHP, and EAHP membranes have been electrospun using the same process parameters, this finding should be imputable to specific solution physical properties changes due to the nonquantitative conjugation of peptide **1** in ELAHA derivative.

As a matter of fact, the acidity of the HFP/H_2O solution should give rise to positively charged ε-amine of Lys residues with a consequent increase of solution conductivity and a reduction in the average diameter. Typically, in fact, the increase of charge density in the electrospun solution affords the formation nanofibers with smaller diameter. In our case, instead, the nonquantitative functionalization of derivative **2** with elastin peptide afforded a low charge density of the solution with a consequent increase of nanofibers diameter.[38]

Overall, the morphology of HP, MAHP and EAHP scaffolds is characterized by the absence of defects and the presence of interconnected nanofibers, which well mimic the ECM three-dimensional structure as well as enable oxygen and vapor permeation in wound dressing applications. These aspects are pivotal for optimal wound dressing design. Moreover, as reported by Kenar and co-workers,[39] the found values of the average fibers diameter of the produced membranes (326 – 569 nm) render the scaffolds good candidates for tissue engineering applications.

Cytotoxicity Assay

A 3-(4,5-dimethylthiazol-2-yl)-5-(3-carboxymethoxyphenyl)-2-(4-sulfophenyl)-2H-tetrazolium (MTS) assay was performed to evaluate the absence of cytotoxicity of the scaffolds. Both with the employment of a methacrylate and methacrylamide moieties in the chemical strategy, the results of the cytotoxicity assay showed no negative influence of the extracts on the metabolic activity of dermal fibroblast cells (Table S1 and Figures S22A-B) After 24 h (Figure S22A), the cells in the extraction medium of scaffold P showed a statistically lower metabolic activity (P = 90 ± 6%) than the medium and the positive gelatin control for *p ≤ 0.05. When pristine HA and methacrylated HA were co-electrospun with PDLLA, a metabolic activity (HP = 95 ± 1% and MHP = 92 ± 5%, respectively) not significantly different to the medium and positive control was reported. In the case of methacrylamidated HA, instead, a statistically lower metabolic activity (MAHP = 91 ± 5%) than the medium and the positive control for *p ≤ 0.05.

The derivative obtained after the conjugation with EL were co-electrospun with PDLLA, and both reported a metabolic activity not statistically different metabolic activity to the medium and the positive control (EHP = 94 ± 5% and EAHP = 96 ± 4).

After 48 h (Figure S22B), all the scaffolds reported a similar metabolic activity to the medium and the positive gelatin control, except MAHP with a value of 85 ± 5% that was statistically different for *p ≤ 0.05 and **p ≤ 0.01.

According to ISO 10993-5:2009, the extract shows no cytotoxic potential if the relative viability is not reduced below 70%. This condition was met in all the scaffolds that were spun out of polymers, which were previously described as mostly biocompatible. No cytotoxicity on fibroblast cells was observed for PDLLA scaffolds and PLA/HA composites.[40]

Conclusion

A semi-synthetic ELAHA bioconjugate has been obtained and described here by exploiting the reactivity of a methacrylamide linker on MAAHA. Simultaneously, because of the low reactivity of the linker, Cys and NAcCys have been investigated in a study on the thiol-Michael addition, where the efficiencies of MAAHA and MAHA have been compared. The study displayed that the different reactivity and efficiency are related to a combination of pH, electron-withdrawing properties of the linkers and the phosphine catalyst excess.

Moreover, to pursue the attractive properties of hyaluronan-elastin materials in wound healing applications, a set of bio-inspired electrospun scaffolds composed of HA, MAAHA, ELAHA, and PDLLA have been produced, evaluating their morphology. The nonquantitative functionalization in the derivative ELAHA affected the morphology, increasing the diameter of the fibers.

At the same time, the cell viability on the electrospun scaffolds has been evaluated, demonstrating the increase of the cells' metabolic activity in the case of the scaffolds containing semi-synthetic derivatives compared to those containing pure HA, even though not significantly.

Experimental section

Materials: Commercial-grade reagents and solvents were used without further purification, except where otherwise indicated. The term "pure H_2O" refers to water purified by a Millipore Milli-Q Gradient system. HA (Mw = 186 KDa) medical device grade was

a generous gift of Altergon Italia SrL. 2-AEMAA·HCl, MTS Assay Kit, 3-(Trimethylsilyl)propionic-2,2,3,3-d_4 acid sodium salt (DSS), NAcCys, Cys, sodium chloride (NaCl), sodium hydroxide pellets (NaOH) were purchased from Sigma Aldrich. HFP and EDC·HCl were purchased from Iris Biotech GmbH, and s-NHS was purchased from TCI Chemicals.
Peptide **1** was synthesized as recently reported.[1] Dulbecco's modified Eagle's medium, fetal bovine serum, penicillin−streptomycin, TCEP·HCl were purchased from ThermoFisher Scientific. PDLLA (EasyFil PLA, transparent pellets, molecular weight: 126 kDa, density: 1240 kg/m^3) was obtained from FormFutura.
Dermal fibroblasts cells (20.000 cells/wel) were purchased from PromoCell.
Dialyses were conducted on Slide-A-LyzerTM Dialysis Cassette G2 2.0 kDa cut-off membranes at 25 °C for MAAHA and MAHA and 3.5 kDa for ELAHA. Freeze-drying was performed with a Christ Alpha 1-4 LD plus freeze-dryer.

NMR spectroscopy: NMR spectra were recorded on 500 MHz (^{1}H: 500 MHz), 400 MHz (^{1}H: 400 MHz, ^{31}P: 162 MHz) Varian Inova instruments in D_2O (DSS 10 mM as internal standard, δ_H = 0 ppm, δ_C = 0 ppm).
COSY experiments were performed using spectral widths of either 3750 Hz in both dimensions, using data sets of 2048×256 points. $DS_{methacryl}$ and $DS_{addition}$ of **2**, **3**, **4**, **5-i,ii**, **6-i,ii**, **7-i,ii** and **8-i,ii** are attributed to disaccharide repeating units.

ATR-FTIR Spectroscopy: ATR spectra were recorded on a model J-460 instrument (Jasco Europe Srl) equipped with an ATR PRO ONE Single-reflection ATR accessory using a single crystal diamond ATR prism. Spectra were acquired in the region from 4000 to 450 cm^{-1} with a spectral resolution of 2 cm^{-1} and 256 scans. Background spectra were recorded each time and then subtracted from the sample spectra.

SEM Analysis: SEM images were acquired with a voltage of 20 kV and different magnifications, after gold sputter-coating on a Philips, FEI ESEM XL30 instrument. The diameter of the fibers was evaluated, on three images for each scaffold, using ImageJ software supplied with the DiameterJ plug-in (n > 100).

MTS Assay: Scaffolds were sterilized during 24 h using UV irradiation (254 nm) then placed in sterile 24-wells plate. Wells containing gelatin coating were coated during 1 h at 37 °C before cells seeding. The fabricated scaffolds were tested for biocompatibility. For this purpose, a cytotoxicity test has been performed using an MTS assay. Each polymer was incubated for 24 h at 37 °C and 5% CO_2 in Dulbecco's modified Eagle's medium and 1% penicillin−streptomycin before seeding cells. Dermal fibroblasts cells were then cultured for 24 h and 48 h on the different scaffolds with sterile cell culture medium supplemented with 10% fetal bovine serum. The cell culture medium alone served as a negative control. Subsequently, the MTS assay was performed according to the manufacturer's protocol (100 µL of MTS were added to each well and incubated for 2 h at 37 °C). The absorbance of the soluble formazan produced by the cellular reduction of MTS was measured at 490 nm (n = 3). The cell viability was determined by the absorption of the samples relative to the control.

General procedure for the Thiol-Michael addition study: The thiol donor and TCEP·HCl were mixed dissolved in pure H_2O obtaining respectively a 32 mM and 47 mM solution. After five minutes it was added to an 8.4 mM solution either of **2** or **4**, and the pH was adjusted to 8.9 with freshly prepared 1.0 M NaOH solution. After 48 h at room temperature the mixture was neutralized with HCl 0.1 M solution and dialyzed against NaCl 150 mM solution for 2 days, and against H_2O for further 2 days. The subsequent freeze-drying yielded a white solid with TCEP=O and TCEP=S as impurities in the derivatives.

Supporting Information

The data that support the finding of this study are available in the supplementary information

Acknowledgements

The authors thank Altergon SrL (Morra De Sanctis, AV, Italy) for hyaluronic acid supply and Mr. Alessandro Laurita (Microscopy Center, University of Basilicata, Potenza, Italy) for SEM images.

Keywords: Elastin; Electrospinning; Hyaluronic acid; MTS Assay; Thiol-Michael reactions.

[1] O. D. Krishna, K. L. Kiick, *Biopolymers* **2020**, *94*, 32-48.
[2] a) J. Hersh, D. Broyles, J. M. C. Capcha, E. Dikici, L. A. Shehadeh, S. Daunert, S. Deo, *ACS Appl. Bio Mater.* **2021**, *4*, 229-251; b) H.-Q. Song, Y. Fan, Y. Hu, G. Cheng, F.-J. Xu, *Adv. Funct. Mater.* **2021**, *31*, 2005978.
[3] T. Mohan, K. S. Kleinschek, R. Kargl, *Carbohydr. Polym.* **2022**, *280*, 118875.
[4] D. P. Nair, M. Podgórski, S. Chatani, T. Gong, W. Xi, C. R. Fenoli, C. N. Bowman, *Chem. Mater.* **2014**, *26*, 724-744.
[5] J. A. Redondo, R. Navarro, E. Martínez-Campos, M. Pérez-Perrino, R. París, J. L. López-Lacomba, C. Elvira, H. Reinecke, A. Gallardo, *J. Polym. Sci. Part A: Polym. Chem.* **2014**, *52*, 2297-2305.
[6] H. Li, B. Li, D. Lv, W. Li, Y. Lu, G. Luo, *Adv. Drug Deliv.* Rev. **2023**, *196*, 114778.
[7] a) E. Shirzaei Sani, R. Portillo-Lara, A. Spencer, W. Yu, B. M. Geilich, I. Noshadi, T. J. Webster, N. Annabi, *ACS Biomater. Sci. Eng.* **2018**, *4*, 2528-2540; b) D. Zhu, H. Wang, P. Trinh, S. C. Heilshorn, F. Yang, *Biomaterials* **2017**, *127*, 132-140; c) M. Wang, Z. Deng, Y. Guo, P. Xu, *Mater. Today Bio* **2022**, *17*, 100495; d) A. Ramamurthi, I. Vesely, *Biomaterials* **2005**, *26*, 999-1010.
[8] a) C. Fiorica, F. S. Palumbo, G. Pitarresi, M. Allegra, R. Puleio, G. Giammona, *J. Drug Del. Sci. Tech.* **2018**, *46*, 28-33; b) F. S. Palumbo, G. Pitarresi, C. Fiorica, S. Rigogliuso, G. Ghersi, G. Giammona, *Mater. Sci. Eng. C Mater. Biol. Appl.* **2013**, *33*, 2541-2549.
[9] M. F. P. Graça, S. P. Miguel, C. S. D. Cabral, I. J. Correia, *Carbohydr. Polym.* **2020**, *241*, 116364.
[10] a) M. Rahmati, D. K. Mills, A. M. Urbanska, M. R. Saeb, J. R. Venugopal, S. Ramakrishna, M. Mozafari, *Prog. Mater. Sci.* **2021**, *117*, 100721; b) C. Gao, L. Zhang, J. Wang, M. Jin, Q. Tang, Z. Chen, Y. Cheng, R. Yang, G. Zhao, *J. Mater. Chem. B* **2021**, *9*, 3106-3130; c) A.

Keirouz, M. Chung, J. Kwon, G. Fortunato, N. Radacsi, *Wiley Inter. Rev. Nanomed. Nanobiotechnol.* **2020**, *12*, e1626; d) A. Memic, T. Abudula, H. S. Mohammed, K. Joshi Navare, T. Colombani, S.A. Bencherif, *ACS Appl. Bio Mater.* **2019**, *2*, 952-969.

[11] a) J. C. Rodriguez-Cabello, I. Gonzalez De Torre, M. Gonzalez-Perez, F. Gonzalez-Perez, I. Montequi, *Front. Bioeng. Biotechnol.* **2021**, *9*, 652384; b) A. Akhmetova, A. Heinz, *Pharmaceutics*, **2021**, *13*, 4; c) D. B. Khadka, M. C. Cross, D. T. Haynie, *ACS Appl. Mater. Interf.* **2011**, *3*, 2994-3001.

[12] H. M. Powell, S. T. Boyce, *Tissue Eng. Part A* **2009**, *15*, 2177-2187.

[13] J. S. Frenkel, *Int. Wound J.* **2014**, *11*, 159-163.

[14] K. C. Castro, M. G. N. Campos, L. H. I. Mei, *Int. J. Biol. Macromol.* **2021**, *173*, 251-266.

[15] C. C. L, Schuurmans, M. Mihaijlovic, C. Hiemstra, K. Ito, W. E. Hennink, T. E. Vermonden, *Biomaterials*, **2021**, *268*, 120602.

[16] a) E. Tsanaktsidou, O. Kammona, C. Kiparissides, *Eur. Polym. J.* **2019**, *114*, 47-56; b) E. J. Oh, J. W. Kim, J. H. Kong, S. H. Ryu, S. K. Hahn, *Bioconj. Chem*. **2008**, *19*, 2401-2408.

[17] E. W. Fowler, A. Ravikrishnan, R. L. Witt, S. Pradhan-Bhatt, X. Jia, *ACS Biomater. Sci. Eng.* **2021**, *7*, 5749-5761.

[18] A. Laezza, A. Casillo, S. Cosconati, C. I. Biggs, A. Fabozzi, L. Paduano, A. Iadonisi, E. Novellino, M. I. Gibson, A. Randazzo, M. M. Corsaro, E. Bedini, *Biomacromolecules*, **2017**, *18*, 2267-2276.

[19] a) A. Laezza, A. Pepe, B. Bochicchio, *Chem. Eur. J.* **2022**, *28*, e202201959; b) G. Piccirillo, A. Pepe, E. Bedini, B. Bochicchio, *Chem. Eur. J.* **2017**, *23*, 2648-2659.

[20] A. Pepe, A. Laezza, A. Ostuni, A. Scelsi, A. Laurita, B. Bochicchio, *Biomimetics*, **2023**, *8*, 193.

[21] G.-Z. Li, R. K. Randev, A. H. Soeriyadi, G. Rees, C. Boyer, Z. Tong, T. P. Davis, C. R. Becer, D. M. Haddleton, *Polym. Chem.* **2010**, *1*, 1196-1204.

[22] J. A. Burns, J. C. Butler, J. Moran, G. M. Whitesides, *J. Org. Chem.* **1991**, *56*, 2648-2650.

[23] T. Kantner, A. G. Watts, *Bioconj. Chem.* **2016**, *27*, 2400-2406.

[24] P. Lee, G. C. Yeo, A. S. Weiss. *FEBS J.* **2017**, *284*, 2216-2230.

[25] J. W. Chan, C. E. Hoyle, A. B. Lowe, M. Bowman, *Macromolecules* **2010**, *43*, 6381-6388.

[26] A. Gennari, J. Wedgwood, E. Lallana, N. Francini, N. Tirelli, *Tetrahedron* **2020**, *76*, 131637.

[27] a) H. Okamoto, T. Taniguchi, M. Takekuma, A. S. Mashio, K. H. Wong, T. Hasegawa, K. Maeda, *Biomacromolecules* **2023**, *24*, 3767-3774; b) S. H. Frayne, B. H. Northrop, *J. Org. Chem.* **2018**, 83, 10370-10382.

[28] K. Cumnock, T. Tully, C. Cornell, M. Hutchinson, J. Gorrell, K. Skidmore, Y. Chen, F. Jacobson, *Bioconj. Chem.* **2013**, *24*, 1154-1160.

[29] Y. J. Lee, Y. Kurra, W. R. Liu, *ChemBioChem* **2016**, *17*, 456-461.

[30] A. Krężel, R. Latajka, G. D. Bujacz, W. Bal, *Inorg. Chem.* **2003**, *42*, 1994-2003.

[31] a) B. H. Northrop, S. H. Frayne, U. Choudhary, *Polym. Chem.* **2015**, *6*, 3415-3430; b) S. Chatani, R. J. Sheridan, M. Podgorski, D. P. Nair, C. N. Bowman, *Chem. Mater*. **2013**, *25*, 3897-3901.

[32] a) G. Tallec, C. Loh, B. Liberelle, A. Garcia-Ac, S. V. Duy, S. Sauvé, X. Banquy, F. Murschel, G. De Crescenzo, *Bioconj. Chem.* **2018**, *29*, 3866-3876; b) Q. Tang, B. Cao, X. Lei, B. Sun, Y. Zhang, G. Cheng, *Langmuir*, **2014**, *30*, 5202-5208.

[33] a) G. B. Desmet, M. M. K. Sabbe, D. R. D'hooge, P. Espeel, S. Celasun, G. B. Marin, F. E. Du Prez, M.-F. Reyniers, *Polym. Chem.* **2017**, *8*, 1341-1352; b) S. Chatani, D. P. Nair, C. N. Bowman, *Polym. Chem.* **2013**, *4*, 1048-1055.

[34] a) N. Ciarfaglia, A. Laezza, L. Lods, A. Lonjon, J. Dandurand, A. Pepe, B. Bochicchio, *J. Appl. Polym. Sci.* **2021**, *138*, e51313; b) N. Ciarfaglia, A. Pepe, G. Piccirillo, A. Laezza, R. Daum, K. Schenke-Layland, B. Bochicchio, *ACS Appl. Polym. Mater.* **2020**, *2*, 4836-4847.

[35] G. R. Williams, B. T. Raimi-Abraham, C. J. Luo, *Nanofibres in Drug Delivery*, UCL Press, London, **2018**, p. 24.

[36] H. Fong, I. Chun, D. H. Reneker, *Polymer* **1999**, *40*, 4585-4592.

[37] S. Tripatanasuwan, Z. Zhong, D. H. Reneker, *Polymer* **2007**, *48*, 5742-5746.

[38] S. O. Han, J. H. Youk, K. D. Min, Y. O. Kang, W. H. Park, *Mat. Lett.* **2008**, *62*, 759-762.

[39] H. Kenar, C. Y. Ozdogan, C. Dumlu, E. Doger, G. T. Kose, V. Hasirci, *Mater. Sci. Eng. C Mater. Biol. Appl.* **2019**, *97*, 31-44.

[40] J. C. Antunes, J. M. Oliveira, R. L. Reis, J. M. Soria, J. L. Gomez-Ribelles, J. F. Mano, *J. Biomed. Mater. Res. Part A* **2010**, *94A*, 856-869.

10.1002/cplu.202300662

WILEY VCH

Entry for the Table of Contents

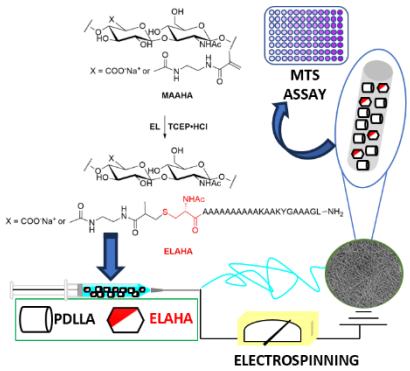

Elastin and hyaluronan have been coupled exploiting a phosphine-mediated thiol-Michael reaction. The conjugate has been blended and electrospun with poly-D,L-lactide (PDLLA), obtaining scaffolds whose morphology and cell viability are influenced by the extent of the peptide coupling. Therefore, the efficiency of the thiol-Michael reaction has been investigated under different conditions.

Institute and/or researcher Twitter usernames: @anto_laezza; @BrigidaBochicc1